RSC Advances

ROYAL SOCIETY OF CHEMISTRY

www.rsc.org/advances

The Effective Adsorption and Decomposition of N_2O on Al-decorated Graphene Oxide under Electric Field

Zhu Lv, Huiyu Mo, Chi Chen*, Xiao Ji, Kui Xu, Ling Miao, Jianjun Jiang

School of Optical and Electronic Information, Huazhong University of Science and Technology, Wuhan, HUBEI 430074, People's Republic of China.

*Email: chenchi_wh89@hotmail.com

Abstract: The adsorption property and decomposition process of N_2O molecule on Al-decorated graphene oxide (Al@GO) are investigated by using first-principles calculations. The physical adsorbed N_2O could be decomposed to N_2 molecule and O atom bonded on Al@GO exothermally (2.33 eV per N_2O molecule), indicating a stronger interaction of Al cation and O anion of N_2O. This interaction will be enhanced with a positive external electric field, inducing the corresponding higher binding energy and shortened $\boldsymbol{d}_{\text{Al-O}}$. The decomposition barrier of N_2O on Al@GO is about 0.50 eV. Especially, for the elongated $\boldsymbol{d}_{\text{Al-O}}$ and shortened $\boldsymbol{d}_{\text{O-N1}}$ in transition state, the decomposition barrier is also decreased monotonously with the increasing electric field. It is remarkable that the N_2O decomposition process becomes almost unimpeded and spontaneous under a positive electric field of 0.50 V/Å. Al-decorated

graphene oxide is expected as a new promising candidate for N_2O decomposition with enhanced adsorption and easier decomposition process.

Keywords: DFT; aluminum; electric field; decomposition barrier; PDOS

1. Introduction

N_2O, which could cause a series of environmental problems like the ozone hole[1] and the greenhouse effect[2], attracts people's attention to investigate its degradation.[3, 4] The decomposition of N_2O into N_2 and O_2 is an eco-friendly way to deal with N_2O gas, as a two-step mechanism of $N_2O \rightarrow N_2 + O$ and $N_2O + O \rightarrow N_2 + O_2$. And the first step is more pivotal, which is focused on by most scholars.[5, 6] In order to overcome the high barrier of N_2O decomposition[7-10], plenty of works have been done to look for appropriate catalysts. Platinum heavy metals[11-16] and some transition metals[17, 18] could effectively decompose N_2O with a relatively low barrier. It is interesting that Al has been found similar catalytic effect with noble metals by A. L. Yakovelv et al.[5]. Especially, I. S. Chopra et al.[19] recently have found that Al could also avoid the shortcomings such as high costs of platinum heavy metals and transition metals while maintaining good catalytic effect.

Graphene oxide (GO) with large specific surface area and good mechanical property is often served as the catalyst substrate.[20] Besides, metal-decorated GO is widely used in gas adsorption and catalytic decomposition.[21-23] In these composites, metal atoms or nano-particles are anchored on GO surface through the oxygen functional groups dispersively and steady. For example, Al-decorated GO could

enhance the adsorption of acid gas and avoid being oxidized at the same time,[23] whose property is extremely effective for the degradation of N_2O in the atmosphere. On the other hand, an external electric field could be a valid measure to adjust the molecule adsorption[24, 25] and bonding state[26-29] on substrate, which could effectively change the corresponding reaction barrier.[10, 30]

In this work, an eco-friendly light metal Al is selected to decorate GO to investigate the process of N_2O decomposition. The relaxed structure of adsorbed state and decomposed state, the binding energy, charge transfer, partial density of state and reaction barrier under different electric fields are carried out to discuss N_2O decomposition.

2. Methods and model

Our first-principles calculations are performed using the SIESTA code[31, 32], based on density functional theory (DFT)[33, 34]. The exchange-correlation energy is calculated within a uniform generalized gradient approximation (GGA) with the Perdew-Burke-Ernzerhof (PBE) functional.[35] We adopt a plane wave cutoff of 150 Ry and a k-point mesh of 4 × 4 × 1 in the Monkhorst-Pack[36] sampling scheme. The structure optimization of adsorbed and decomposed states is performed by relaxing the forces on all the atoms until the convergence precision of the forces is less than 0.02 eV/Å.

Al-decorated GO is adopted as the substrate to investigate the adsorption and decomposition processes of N_2O. Based on the well-known GO model proposed by A.

Lerf and J. Klinowski[37, 38], recently our former research has found two relatively stable configurations of Al-decorated GO with adjacent double epoxies or adjacent double hydroxyls (type I and II shown in Figure 1).[23] In this work, a 4 × 4 × 1 hexagonal graphene supercell containing 32 carbon atoms is used as the initial model for GO, as shown in Figure 1 (a). And we place GO in the ***xy*** plane (9.840 Å × 9.840 Å) and set the translation vector along ***z*** direction as 18 Å to ensure that no interaction occurs between the adjacent cell systems.

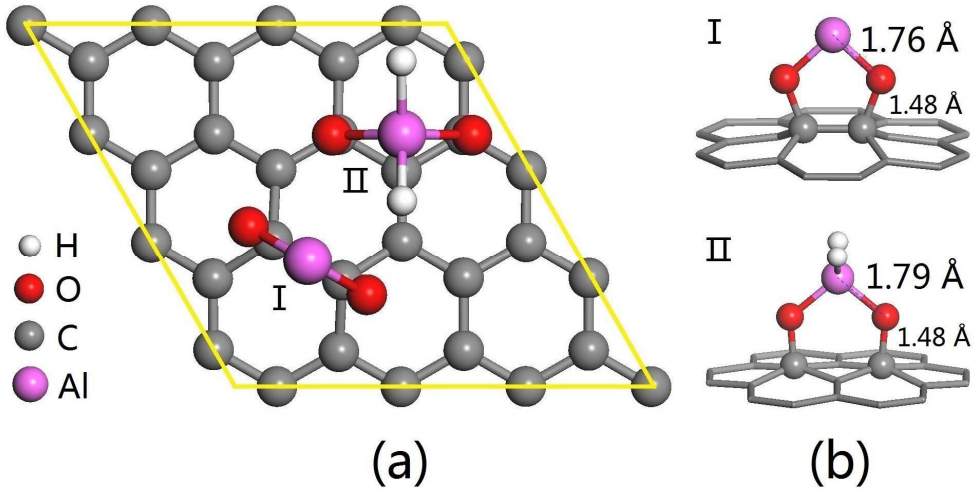

Figure 1. (a) The front views of type I and type II, (b) the plan views of type I and type II.

3. Results and discussion

3.1 N_2O adsorption

Ⅰ The adsorption of N_2O on Al-decorated GO

Our calculations show that N_2O could be absorbed stably on the type I site of Al-decorated GO, while there is no steady state that N_2O could be absorbed on the

type II site, as the hydrogen atoms passivation will weaken the chemical activity of Al atom on the substrate. Therefore, Al-decorated GO with adjacent double epoxies named Al@GO is selected in the following investigations. At the same time, the Al metal diffusion and clustering would not occur on the Al@GO system through our verification.

The adsorption of N_2O molecule on Al@GO is investigated in two configurations according to the orientation of N_2O, labeled as O-end and N-end structures as shown in Figure 2. The binding energy $\boldsymbol{E}_b$ of N_2O on Al@GO is defined as

$$\boldsymbol{E}_b = \boldsymbol{E}_{tot} - (\boldsymbol{E}_{substrate} + \boldsymbol{E}_{gas}),$$

where $\boldsymbol{E}_{tot}$ is the total energy of Al@GO with an adsorbed N_2O molecule, and $\boldsymbol{E}_{substrate}$, $\boldsymbol{E}_{gas}$ are total energies of Al@GO and N_2O molecule, respectively.

The binding energy of N_2O on Al@GO through O-end is −0.25 eV, which is increased significantly compared with N_2O on pristine graphene (−0.07 eV)[10] and similar to that of $Al(OH)_3(H_2O)_2$ (−0.23 eV)[5]. The distance between Al and O atom of N_2O molecule is 2.76 Å and the lengths of N1-N2 and O-N1 bonds are almost unchanged, suggesting that the physical adsorption of N_2O on Al@GO is a kind of electrostatic interaction. It agrees with the population analysis[39, 40] as plotted in Figure 2 (b). An electrical dipole moment is formed between O atom (0.29 $\boldsymbol{e}$) and Al atom (−1.96 $\boldsymbol{e}$), resulting in a relatively strong electrostatic interaction of N_2O molecule and Al@GO.

N_2O molecule could be decomposed into N_2 molecule and O_{ad} atom bonded on

the Al@GO system. As shown in Figure 2 (a), the distance of Al atom and O atom is 1.67 Å, showing a strong chemical bond forms between them. Besides, the distance between N_2 molecule and O atom is 2.93 Å while the bond length of N1-N2 is almost unchanged compared to the previous adsorbed state, leading to a Van der Waals adsorption of N_2 molecule on O-Al@GO substrate. The above structural changes reflect old O-N1 bond rupture and new Al-O bond formation in whole system. In addition, the relative energy of the decomposed state is 2.33 eV lower than that of the adsorbed state, indicating a stronger interaction of Al-O bond than that of O-N1 bond. Synthesizing these analyses, we could look forward to a relatively low decomposition barrier in this reaction.

While N_2O molecule is adsorbed on the Al@GO through N-end, we could get the similar adsorbed structure with a slightly higher relative energy (0.06 eV). However, the relative energy of the corresponding decomposed state, in which Al-N bond forms and N-N bond ruptures, is 3.46 eV higher than that of the adsorbed state. It means the decomposition reaction of N_2O through N-end on the Al@GO is endothermic, and difficult to occur. So, our following works mainly focus on the adsorption and decomposition process of N_2O on the Al@GO through O-end.

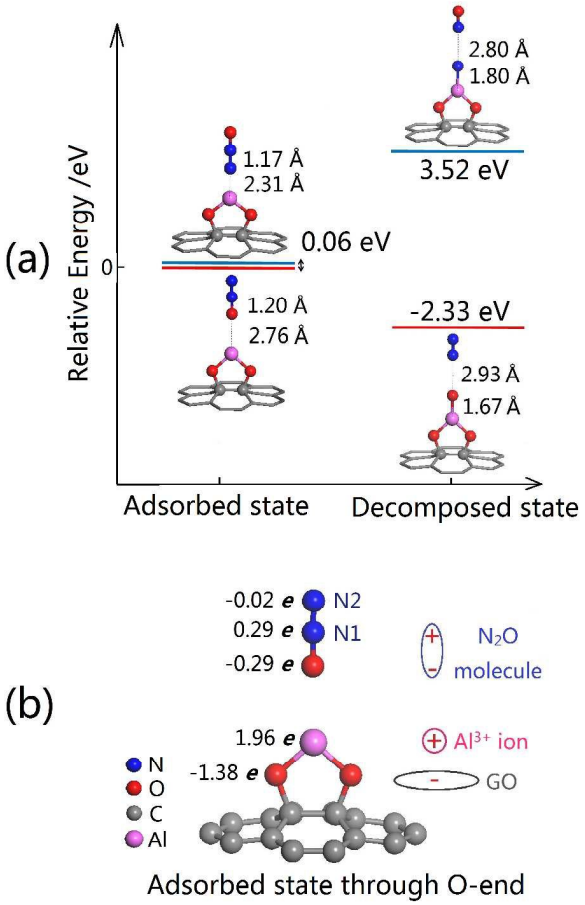

Figure 2. The relative total energies of adsorbed state and decomposed state through N-end and O-end, and the bader charge of adsorbed state through O-end.

Ⅱ The adsorption of N_2O under electric field

Since an electrical dipole moment ***P*** exists between N_2O molecule and Al@GO as mentioned above, a series of electric fields ***E*** are applied to the adsorbed state to investigate the effect of external electric fields on the binding energy. The perpendicular ***E*** ranges from −0.50 to 0.50 V/Å with a step of 0.25 V/Å. As shown in Figure 3 (a), the calculated binding energy E_b increases monotonously ranging from 0.14 eV to 0.64 eV with increasing ***E***, which means that a positive electric field could

enhance the interaction between N_2O molecule and Al@GO. Meanwhile, as shown in Figure 3 (b), the corresponding $\boldsymbol{d}_{Al\text{-}O}$ is monotonously shortened from 3.24 Å to 2.09 Å and $\boldsymbol{d}_{O\text{-}N1}$ is lengthened from 1.19 Å to 1.24 Å, indicating an enhanced interaction of Al atom and O atom with increasing $\boldsymbol{E}$.

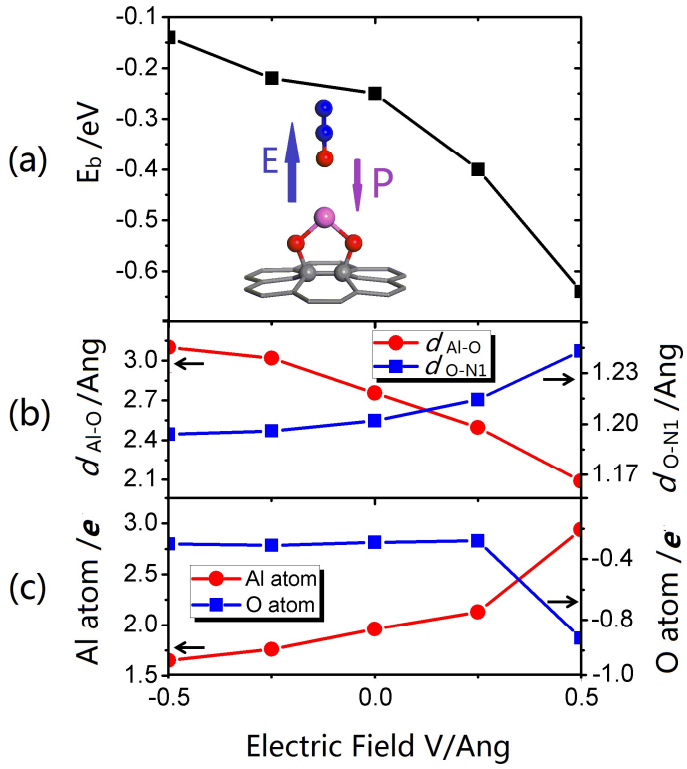

Figure 3. (a) The binding energies of N_2O on Al@GO, (b) $\boldsymbol{d}_{Al\text{-}O}$ and $\boldsymbol{d}_{O\text{-}N1}$, (c) the bader charges of Al atom and O atom in adsorbed states under different electric fields. The legend is the same as Figure 2.

The variations of binding energy and the bond length could be resulted from two dominant factors: the interaction between inherent electric dipole $\boldsymbol{P}$ with $\boldsymbol{E}$ and the charge redistribution induced by $\boldsymbol{E}$. The formula $W= -\boldsymbol{P}\times\boldsymbol{E}$ means a stronger interaction with increasing $\boldsymbol{E}$. On the other hand, according to bader charge analysis, the charge of O atom is almost unchanged at the beginning, while the charge of Al

atom increases monotonously with increasing ***E***, as shown in Figure 3(c). A greater electric dipole ***P*** induced by the charge transfer could also enhance the interaction between N_2O molecule and Al@GO.

It is noteworthy that when ***E*** = 0.50 V/Å, the charge of O atom and Al atom changes suddenly. The corresponding $\boldsymbol{d}_{\text{O-N1}}$ (1.24 Å) and $\boldsymbol{d}_{\text{Al-O}}$ (2.09 Å) indicate that the old O-N1 bond is weakened significantly and a new Al-O bond is formed. The coexistence of O-N1 and Al-O bonds in the relaxed adsorbed state is very similar to the characteristic of transition state in decomposition process. Thus the structural transformation from adsorbed state to transition state is favorable with a lower energy barrier under an appropriate electric field.

3.2 N_2O decomposition

Ⅰ The decomposition process of N_2O

We next investigate the decomposition process of N_2O molecule on the Al@GO structure and the calculated decomposition barrier and route are obtained in Figure 4 (a). The interesting thing is that the decomposition barrier ($\Delta \boldsymbol{E}$) is only 0.50 eV, which is comparable to traditional platinum group metals catalysts, as its $\Delta \boldsymbol{E}$ is from 0.32 eV to 0.84 eV. [41-43]

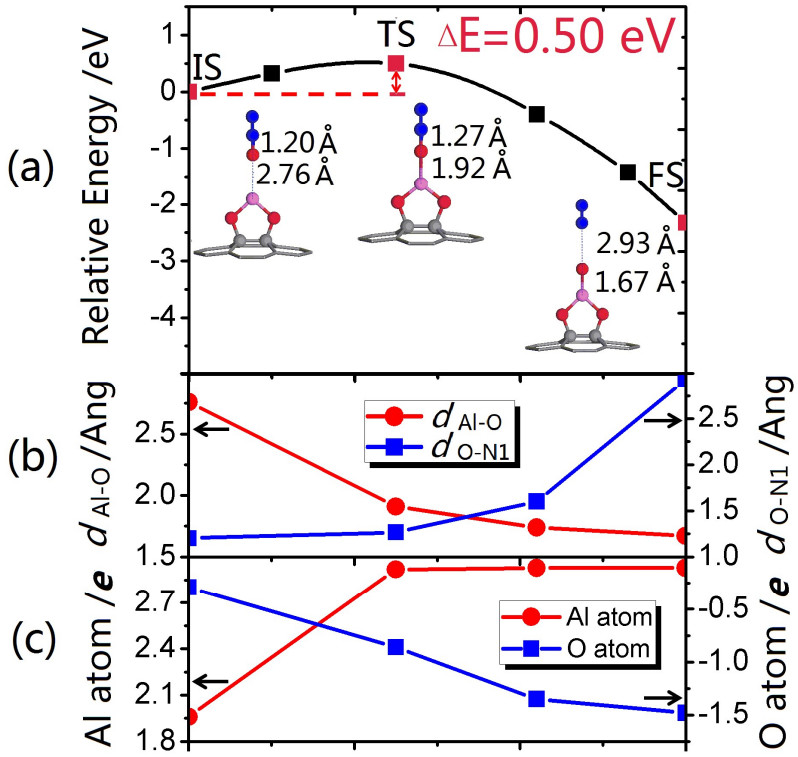

Figure 4. (a) Minimum-energy pathway via the $N_2O \rightarrow N_2 + O_{ad}$ route, (b) the variations of $\boldsymbol{d}_{Al\text{-}O}$ and $\boldsymbol{d}_{O\text{-}N1}$ in the decomposition process, (c) the bader charges of Al atom and O atom in the decomposition process. The legend is the same as Figure 2.

It's important to understand the reaction process and the N_2O decomposition mechanism. Here, the initial state, the transition state and the final state are noted as IS, TS and FS, respectively in the following discussion. With the reaction proceeding, $\boldsymbol{d}_{Al\text{-}O}$ is shortened while $\boldsymbol{d}_{O\text{-}N1}$ is elongated gradually, especially when it comes to TS. Compared with IS, $\boldsymbol{d}_{Al\text{-}O}$ of TS is shortened from 2.76 Å to 1.92 Å, meanwhile $\boldsymbol{d}_{O\text{-}N1}$ is lengthened 0.07 Å as shown in Figure 4 (b), which means the structure of N_2O molecule has been effected and the interaction between Al atom and O atom is strengthened significantly. According to bader charge analysis, the charge transfer

mainly occurs in the process from IS to TS, where Al acting as a bridge could transfer the charges from the substrate to N_2O molecule. While there is almost no charge redistribution from TS to FS in Figure 4 (c), suggesting the structure of TS is close to the stable FS.

The barrier of N_2O decomposition process on the Al@GO structure (0.50 eV) is lower than that of $Al(OH)_3(H_2O)_2$ (0.87 eV), [5] suggesting the reaction on the Al@GO structure could perform more easily. Al atom acts as the catalytic site in both structures, and the chemical state of Al atom is the dominated factor for energy barrier of N_2O decomposition. Meanwhile, different chemical environments will influence the valence and the chemical activity of Al atom significantly. So, the chemical activity of the Al atom surrounded by three hydroxyl groups in $Al(OH)_3(H_2O)_2$ is weakened severely because of small effective contact area with N_2O molecule. In comparison, Al atom in Al@GO structure only forms a bond with two oxygen atoms of the substrate respectively， with relatively larger effective contact area exposed. On the other hand, the reaction heat of N_2O decomposed process on the Al@GO structure (2.33 eV) is larger than that of $Al(OH)_3(H_2O)_2$ (0.77 eV), which also shows that it is more favorable for N_2O to be decomposed on the Al@GO structure.

In order to further investigate the electronic hybridization behavior of N_2O decomposition on the Al@GO, the partial density of state (PDOS) for three states (IS, TS and FS) are plotted in Figure 5. As shown in Figure 5 (a), there are two overlapped hybridization orbital peaks between O-2p and N1-2p at about −8.00 eV and 3.00 eV, indicating that the O atom and N1 atom are still strong covalent bond. While the result

that almost no overlapped hybridization orbital peaks between O-2p and N1-2p in Figure 5 (c) proves that the covalent bond between O atom and N1 atom has been fractured in FS. Specially, the PDOS of TS in Figure 5 (b) shows the overlapped hybridization orbital peaks between O-2p and Al-3p is weaker than that of FS and the similar peaks between O-2p and N1-2p is weaker than that of IS, suggesting that a new Al-O bond is formed and the old O-N1 bond is fractured gradually.

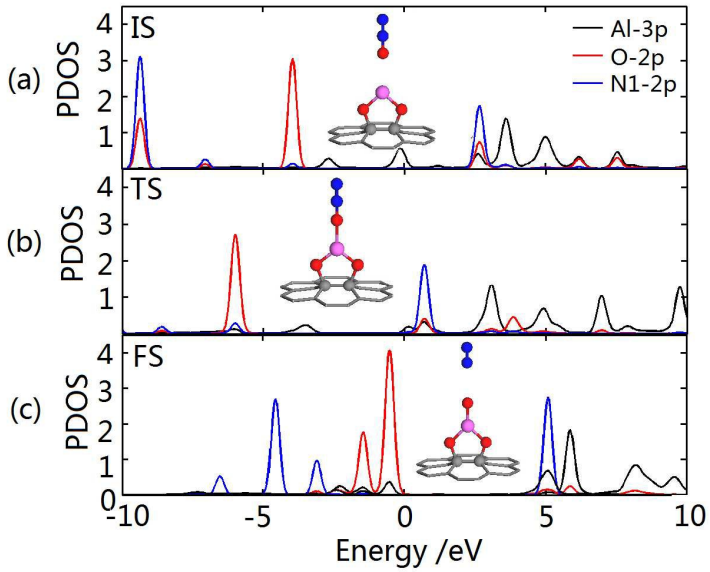

Figure 5. PDOS of IS, TS and FS during N_2O decomposition process on the Al@GO system. The legend is the same as Figure 2.

Ⅱ The decomposition of N_2O under electric field

The decomposed states under electric fields are obtained in Figure 6. The results show that the bond of Al-O_{ad} is slightly lengthened from 1.66 Å to 1.67 Å, and the binding energy of N_2 molecule on the O_{ad}-Al@GO state almost keeps unchanged with the applied electric field ranging from −0.50 V/Å to 0.50 V/Å, indicating the electric field mainly have effects on the adsorbed state instead of the decomposed state.

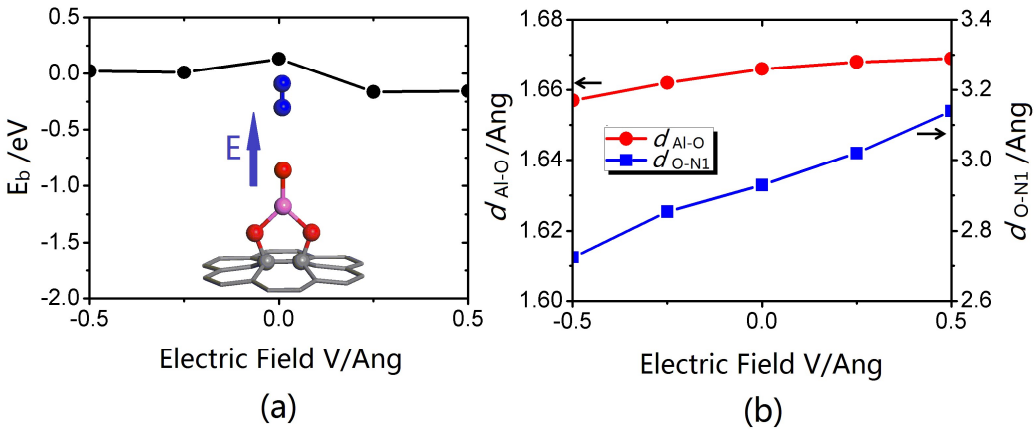

Figure 6. (a) The binding energies, (b) $d_{Al\text{-}O}$ and $d_{O\text{-}N1}$ in decomposed states under different electric fields. The legend is the same as Figure 2.

Considering the analysis of the decomposition barrier could contribute to understanding the role that electric field plays in the process of N_2O decomposition, we calculate the decomposition barrier under each electric field. As shown in Figure 7, the decomposition barrier is decreased monotonously with $\boldsymbol{E}$ varies from −0.50 V/Å to 0.50 V/Å. It is worth noting that up to $\boldsymbol{E}$ = 0.50 V/Å, the barrier is almost nonexistent, as the corresponding barrier drops to only 0.02 eV. What is more, when $\boldsymbol{E}$ is slightly larger than 0.50 V/Å, the O-N1 bond is fractured with no barrier and the spontaneous decomposition of N_2O on Al@GO could be realized.

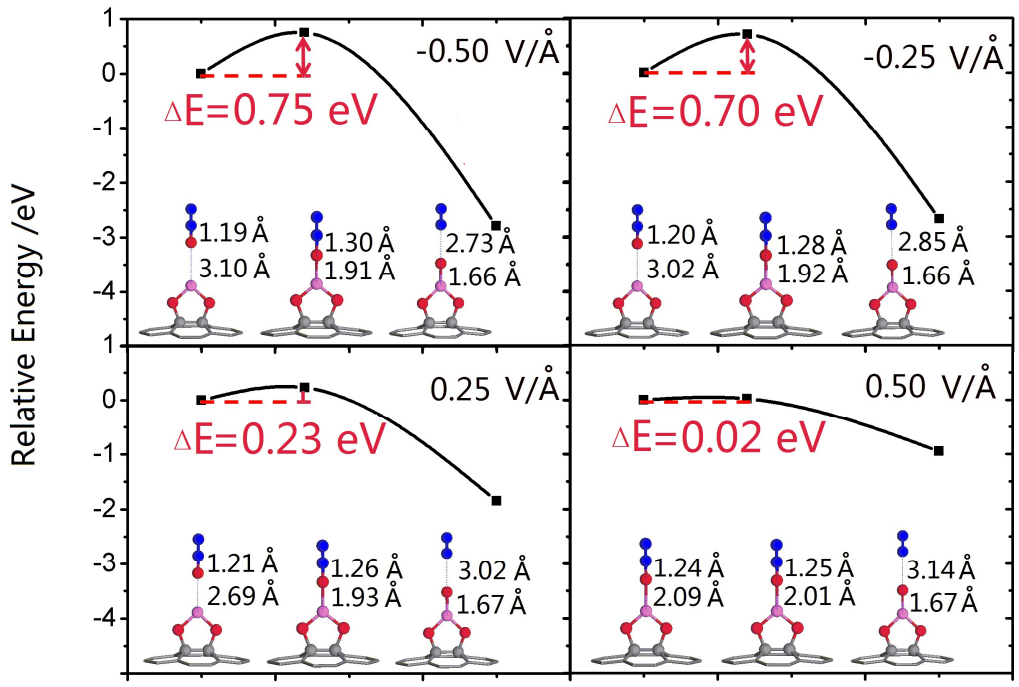

Figure 7. The decomposition barriers and IS, TS, FS under different electric fields. The legend is the same as Figure 2.

To further study the decomposition barrier variation, we investigate IS, TS and FS under different ***E***, as plotted in Figure 7. As for TS, $d_{\text{Al-O}}$ increases monotonously while $d_{\text{O-N1}}$ decreases monotonously with the increasing ***E***. What is more, the structure of IS is more similar to that of TS, contributing to the decrease of the decomposition barrier.

The PDOS of IS, TS and FS under different electric fields are plotted in Figure 8. The results show that the PDOS of every TS and FS almost keeps unchanged while that of corresponding IS performs some different characteristics, indicating that electric field has relatively greater influence on IS. Furthermore, when ***E*** = 0.50 V/Å, the PDOS of IS with overlapped Al-3p and O-2p orbital peaks is more analogous to that of TS, which is consistent with the similarity of their structures. As analyzed

above, the electric field could indeed promote the catalytic decomposition of N_2O into N_2 and O_{ad} on the Al@GO system.

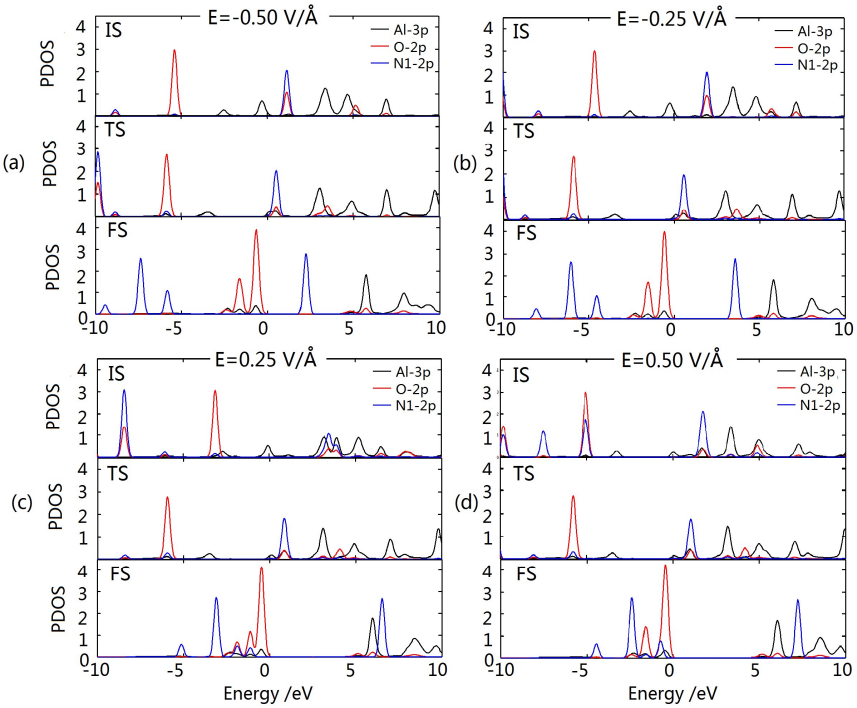

Figure 8. PDOS of IS, TS and FS under different electric fields on the Al@GO system.

4. Conclusions

In summary, the adsorption property and decomposition process of N_2O molecule on Al@GO are investigated by using first-principles calculations. N_2O molecule will be adsorbed on Al@GO through O-end and an electrical dipole moment is formed between O atom (0.29 e) and Al atom (−1.96 e), resulting in a relatively strong electrostatic interaction of N_2O molecule and Al@GO with binding energy of −0.25 eV. Also, Al@GO is demonstrated to be benefit to N_2O decomposition with much lower barrier of 0.50 eV. What is more, the adsorption and decomposition of N_2O on the Al@GO will be enhanced with the increasing of a positive external electric field.

It should be noted that the N_2O decomposition process becomes almost unimpeded and spontaneous under a positive electric field of 0.50 V/Å with barrier of 0.02 eV. On the other hand, Van der Waals correction has been taken into consideration. And the results indicate that the influence of Van der Waals interactions may be relatively small and the main conclusions above remain. Thus, our work provides an efficient and economic method to capture and decompose N_2O gas.

Acknowledgements

This research work is supported by National Natural Science Foundation of China (Grant No. 51302097), Wuhan Planning Project of Science and Technology (No. 2013011801010594), the Fundamental Research Funds for the Central Universities, HUST (Grant No. CXY13Q003). Computational resources provided by Center of Computational Material Design and Measurement Simulation, Huazhong University of Science and Technology are gratefully acknowledge.

Reference

1 A. R. Ravishankara, J. S. Daniel, and R. W. Portmann, *Science*, 2009, **326**, 123–125.

2 J. Hansen and M. Sato, *Proc. Natl. Acad. Sci. U.S.A.*, 2004, **101**, 16109−16114.

3 D. J. Wuebbles, *Science*, 2009, **326**, 56.

4 D. J. Beerling, A. Fox, D. S. Stevenson, and P. J. Valdes, *PNAS*., 2011, **108**, 9770–9775.

5 A. L. Yakovlev and G. M. Zhidomirov, *Catalysis letters*, 1999, **63**, 91-95.

6 E. V. Kondratenko and J. Pérez-Ramírez, *Catalysis Letters*, 2003, **91**, 3-4.

7 F. Kapteijn, J. Rodriguez-Mirasol, and J. A. Moulijn, *Appl. Catal. B*, 1996**, 9,** 25–64.

8 V. K. Tzitzios and V. Georgakilas, *Chemosphere*, 2005, **59**, 887−891.

9 J. P. Dacquin, C. Dujardin, and P. Granger, *J. Catal.*, 2008, **253**, 37−49.

10 Y. Lv, G. Zhuang, J. Wang, Y. Jia, and Q. Xie, *Phys. Chem. Chem. Phys.*, 2011, **13**, 12472−12477.

11 S. Haq and A. Hodgson, *Surf. Sci.*, 2000, **463**, 1−10.

12 A. Kokalj, I. Kobal, H. Horino, Y. Ohno, and T. Matsushima, *Surf. Sci.*, 2002, **506**, 196−202.

13 R. Burch, S. T. Daniells, J. P. Breen, and P. Hu, *J. Catal*.,2004**, 224**, 252−260.

14 A. Kokalj and T. Matsushima, *J. Chem. Phys.*, 2005, **122**, 034708.

15 F. Rondinelli, N. Russo, and M. Toscano, *J. Chem. Theory Comput.*, 2008, **4**, 1886−1890.

16 X. Wei, X. F. Yang, A. Q. Wang, L. Li, X. Y. Liu, T. Zhang, C. Y. Mou, and J. Li, *J. Phys. Chem. C*, 2012, **116**, 6222−6232.

17 A. Stirling, *J. Am. Chem. Soc.*, 2002, **124**, 4058−4067.

18 H. Orita and N. Itoh, *Surf. Sci.*, 2004, **550**, 166−176.

19 I. S. Chopra, S. Chaudhuri, J. F. Veyan, and Y. J. Chabal, *Nature Materials*, 2011, **10**, 884–889.

20 S. Stankovich, D. A. Dikin, R. D. Piner, K. A. Kohlhaas, A. Kleinhammes, Y. Jia, Y. Wu, S. T. Nguyen, and R. S. Ruoff, *Carbon*, 2007, **45**, 1558–1565.

21 L. Wang, K. Lee, Y. Y. Sun, M. Lucking, Z. Chen, J. J. Zhao, and S. B. Zhang, *ACS Nano*, 2009, **3**, 2995–3000.

22 L. Wang, J. Zhao, L Wang, T Wang, Y. Sun, and S. B. Zhang, *Phys. Chem. Chem. Phys.*, 2011, **13**, 21126–21131.

23 C. Chen, K. Xu, X. Ji, L. Miao, and J. Jiang, *Phys. Chem. Chem. Phys.*, 2014, **16**, 11031-11036.

24 W. Liu, Y. H. Zhao, Y. Li, E. J. Lavernia, and Q. Jiang, *Phys. Chem. Chem. Phys.*, 2009, **11**, 9233–9240.

25 Z. M. Ao and F. M. Peeters, *Appl. Phys. Lett.*, 2010, **96**, 253106.

26 C. He, P. Zhang, Y. F. Zhu, and Q. Jiang, *J. Phys. Chem. C*, 2008, **112**, 9045-9049.

27 W. Liu and Q. Jiang, *J. Comput. Theor. Nanosci.*, 2010, **7**, 2225-2261.

28 N. Liu, B. Chen, Y. Li, R. Zhang, X. Liang, Y. Li, and Z. Lei, *J Phys. Chem. C*, 2011, **115**, 12883–12890.

29 C. Chen, L. Miao, K. Xu, J. Yao, C. Li, and J. Jiang, *Phys. Chem. Chem. Phys.*, 2013, **15**, 6431—6436.

30 E. H. Song, J. M. Yan, J. S. Lian, and Q. Jiang, *J. Phys. Chem. C*, **2012**, *116*,

20342–20348.

31 J. M. Soler, E. Artacho, J. D. Gale, A. Garcı′a, J. Junquera, P. Ordejo′n, and D. Sa′nchez-Portal, *J. Phys. Condens. Matter*., 2002, **14**, 2745.

32 G. Roma′n-Pe′rez and J. M. Soler, *Phys. Rev. Lett*., 2009, **103**, 096102.

33 P. Hohenberg and W. Kohn, *Phys. Rev.*, 1964, **136**, B864.

34 W. Kohn and L. J. Sham, *Phys. Rev.*, 1965, **140**, A1133–A1138.

35 B. Hammer, L. B. Hansen, and J. K Nørskov, *Phys. Rev. B*, 1999, **59**, 7413–7421.

36 H. J. Monkhorst and J. D. Pack, *Phys. Rev. B*, 1976, **13**, 5188–5192.

37 A. Lerf, H. He, M. Forster, and J. Klinowski, *J. Phys. Chem. B*, 1998, **102**, 4477–4482.

38 H. He, J. Klinowski, M. Forster, and A. Lerf, *Chem. Phys. Lett.*, 1998, **287**, 53 – 56.

39 W. Tang, E. Sanville, and G. Henkelman, *J. Phys.: Condens. Matter*, 2009, **21**, 084204.

40 E. Sanville, S. D. Kenny, R. Smith, and G. Henkelman, *J. Comput. Chem.*, 2007, **28**, 899-908.

41 V. A. Kondratenko and M. Baerns, *J. Catal.*, 2004, **225**, 37–44.

42 J. F. Paul, J. P. Ramírez, F. Ample, and J. M. Ricart, *J. Phys.Chem. B*, 2004, **108**, 17921–17927.

43 J. M. Ricart, F. Ample, A. Clotet, D. Curulla, J. W. Niemantsverdriet, J. F. Paul, and J. Pérez-Ramírez, *J. Catal*., 2005, **232**, 179–185.

Figures list

Figure 1. (a) The front views of type I and type II, (b) the plan views of type I and type II.

Figure 2. The relative total energies of adsorbed state and decomposed state through N-end and O-end, and the bader charge of adsorbed state through O-end.

Figure 3. (a) The binding energies of N_2O on Al@GO, (b) $\boldsymbol{d}_{Al\text{-}O}$ and $\boldsymbol{d}_{O\text{-}N1}$, (c) the bader charges of Al atom and O atom in adsorbed states under different electric fields. The legend is the same as Figure 2.

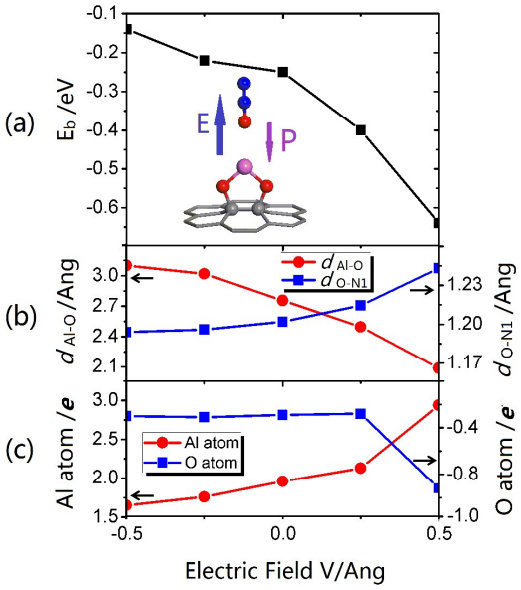

Figure 4. (a) Minimum-energy pathway via the $N_2O \rightarrow N_2 + O_{ad}$ route, (b) the variations of $\boldsymbol{d}_{Al\text{-}O}$ and $\boldsymbol{d}_{O\text{-}N1}$ in the decomposition process, (c) the bader charges of Al atom and O atom in the decomposition process. The legend is the same as Figure 2.

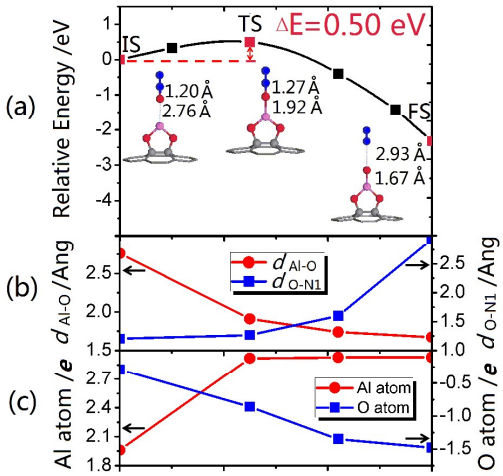

Figure 5. PDOS of IS, TS and FS during N_2O decomposition process on the Al@GO system. The legend is the same as Figure 2.

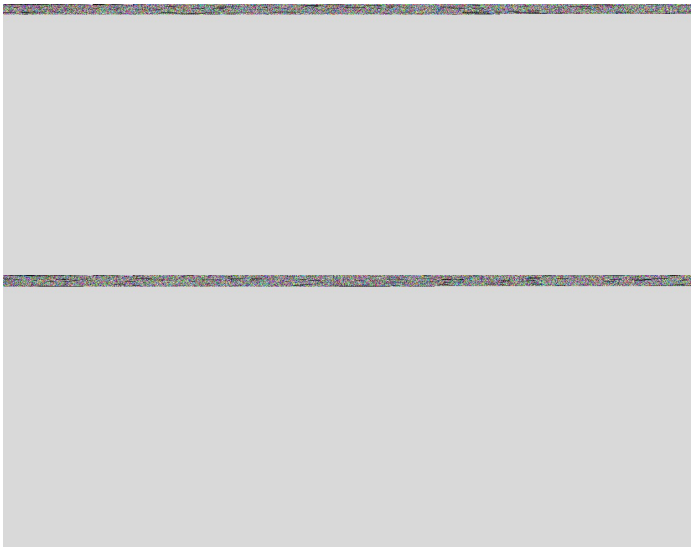

Figure 6. (a) The binding energies, (b) $d_{Al\text{-}O}$ and $d_{O\text{-}N1}$ in decomposed states under different electric fields. The legend is the same as Figure 2.

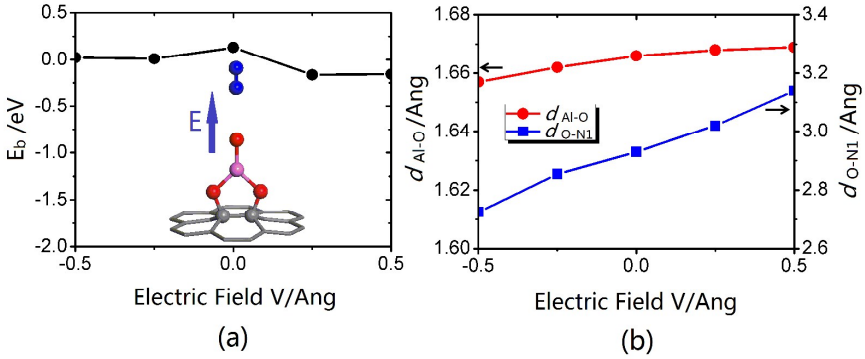

Figure 7. The decomposition barriers and IS, TS, FS under different electric fields. The legend is the same as Figure 2.

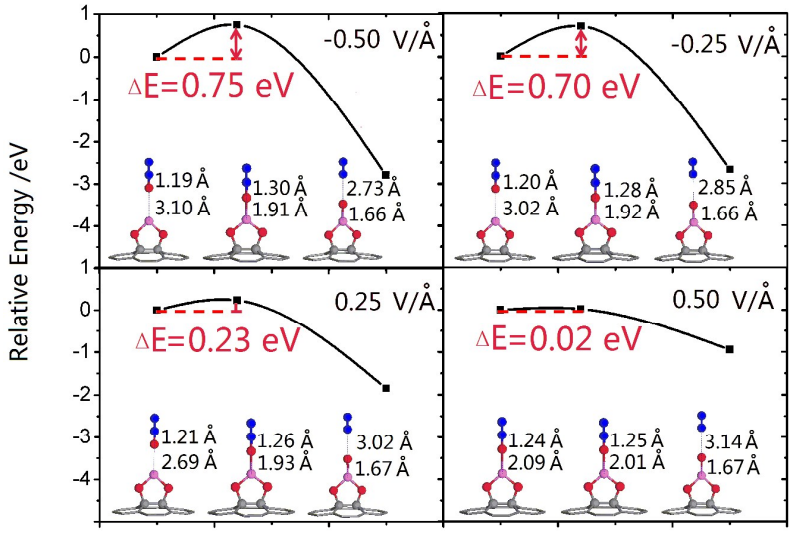

Figure 8. PDOS of IS, TS and FS under different electric fields on the Al@GO system.

TOC

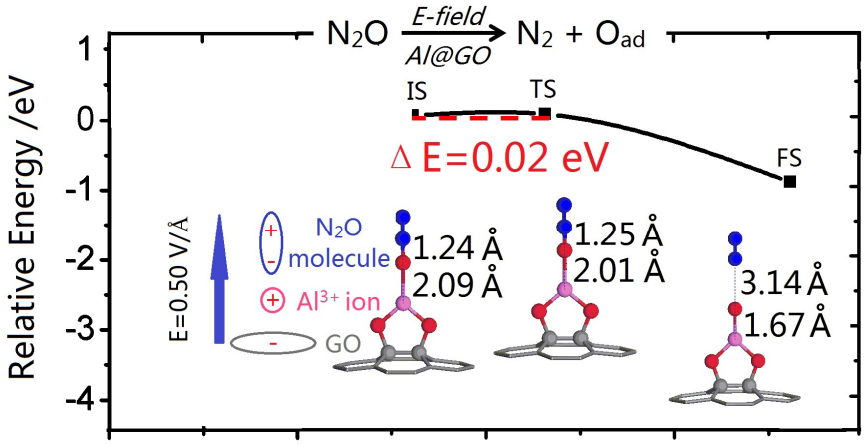

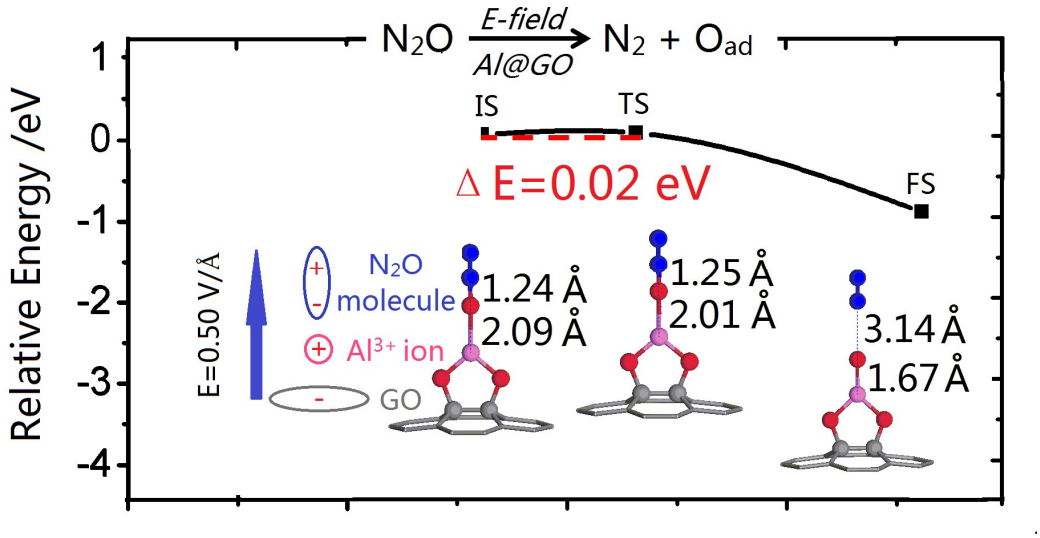

Al-decorated graphene oxide is expected as a new promising candidate for N_2O decomposition with enhanced adsorption and easier decomposition process.